

Young stellar objects from soft to hard X-rays

Manuel Güdel

Institute of Astronomy, ETH Zurich, 8093 Zurich, Switzerland

Abstract. Magnetically active stars are the sites of efficient particle acceleration and plasma heating, processes that have been studied in detail in the solar corona. Investigation of such processes in young stellar objects is much more challenging due to various absorption processes. There is, however, evidence for violent magnetic energy release in very young stellar objects. The impact on young stellar environments (e.g., circumstellar disk heating and ionization, operation of chemical networks, photoevaporation) may be substantial. Hard X-ray devices like those carried on Simbol-X will establish a basis for detailed studies of these processes.

Keywords: Star formation, young stellar objects, X-ray emission, hard X-rays, non-thermal X-rays

PACS: 95.85.Nv, 97.10.Bt, 97.10.Ex, 97.10.Jb, 97.21.+a

INTRODUCTION

X-ray radiation from young stars are fundamentally important for molecular stellar environments. X-rays ionize protostellar envelopes and circumstellar disks [14]. In the presence of weak magnetic fields, ionized disk surface layers grow unstable to the magnetorotational instability [3], currently accepted as the most promising driver of accretion through disks. Further, X-ray irradiation of circumstellar molecular gas drives important chemistry, including production or destruction of water [15, 43]. X-rays heat disk surfaces to temperatures of several thousand K [15], giving rise to (partial) photoevaporation of, and therefore mass loss from, the innermost disk regions [9].

Stellar X-ray astronomy has concentrated on the *soft* X-ray range (SXR, ≈ 0.1 – 10 keV), where *thermal* bremsstrahlung and line radiation dominate. Harder X-rays >10 keV (HXR) are somewhat of a *terra incognita* in stellar astronomy, notwithstanding a few firm detections beyond ≈ 20 keV and marginal claims for detections of non-thermal HXR. Simbol-X promises a breakthrough for stellar HXR, thus opening a window to deeply embedded, young X-ray sources and to the physics of magnetic energy release in young, magnetically active stars [1, 31, 32, 33, 41].

MAGNETIC FIELDS IN PROTOSTARS?

It is essentially unknown when during star formation *stellar* magnetic fields first appear, and whether they are fossil or are generated by internal dynamos. Our understanding of magnetic-field induced high-energy environments of the youngest stars is very limited.

A rather comprehensive picture of the X-ray characteristics of T Tauri stars (TTS) is available, especially from large recent surveys with XMM-Newton and Chandra [12, 20, 40]. In short, TTS X-ray emission mostly originates from magnetic coronae, with characteristics similar to more evolved active main-sequence stars. Their X-rays saturate

at a level of $\log(L_X/L_{\text{bol}}) \approx -3.5$. Because for a typical pre-main sequence association L_{bol} roughly correlates with stellar mass M_* , one also finds a distinct correlation between L_X and M_* , $\log L_X \propto M_*^{1.7 \pm 0.1}$ [45]. Flaring is common in TTS [44], the most energetic examples reaching temperatures of $\approx 10^8$ K [25].

The complex stellar environments of protostars and TTS may lead to further X-ray sources. Accretion streams may form shocks at the stellar surface, producing very soft X-rays. The evidence is twofold: unusually high electron densities have been inferred from spectral line ratios from a handful of TTS [27], and a general “soft excess”, defined by an anomalously high ratio of O VII $\lambda 21.6$ to O VIII $\lambda 19.0$ line fluxes [17]. Jets and outflows may shock heat some gas to >1 MK, both in Herbig-Haro objects far away from the driving stars [37] and internal to jets very close to the stars [21]. These X-ray sources are also soft, typically detected only below ≈ 1 -2 keV. This is not surprising given the energy available from shock velocities of no more than a few hundred km s^{-1} .

The picture is much less complete for earlier phases of star formation owing to strong X-ray attenuation. Non-thermal radio emission from Class I protostars suggests the presence not only of magnetic fields but also accelerated particles, both in distant regions of outflows (e.g., [39]) and within the stellar corona [42].

For “Class 0 objects” (the earliest phase of a forming star), a few promising candidates but no definitive cases have been reported (e.g., [22]). Giardino et al. [13] summarize several Class 0 non-detections, with a “stacked Class 0 data set” corresponding to 540 ks of Chandra ACIS-I exposure time still giving no indication for a detection. In the absence of detailed information on the absorbing gas column densities or the intrinsic spectral properties, an interpretation within an evolutionary scenario is difficult.

The situation is more favorable for more evolved Class I protostars although sample statistics are biased by strong X-ray attenuation, favoring detection of the most luminous and the hardest sources. A comprehensive study is available for the Orion region [38]. The X-ray luminosities increase from protostars to TTS by about an order of magnitude, although the situation is unknown below 1-2 keV. No significant trend is found for the electron temperatures, which are similarly high (≈ 1 -3 keV) for all detected classes.

Protostellar HXR detections with Simbol-X will be particularly interesting: emission above ≈ 5 – 10 keV is mostly unabsorbed, permitting unbiased studies of deeply embedded protostars, thus pinpointing the earliest appearance of magnetic activity and high-energy stellar environments. Such observations will also be crucial to understand magnetic energy release in these youngest objects, as discussed below.

FLARE PHYSICS IN YOUNG STARS

Magnetic energy release and the ensuing electromagnetic spectrum have been studied in detail for the solar corona [8, 30]. The standard flare scenario posits that non-potential coronal magnetic fields reconnect and thus release kinetic and thermal energy. While traveling along closed magnetic fields and colliding in denser chromospheric layers, accelerated particles emit prompt gyrosynchrotron, optical, and ultraviolet radiation and non-thermal hard X-rays. The energy deposition explosively heats gas to >10 MK, and the resulting overpressure drives the newly heated gas along the magnetic field lines into the corona. Soft X-rays are emitted by the hot plasma accumulating in coronal loops,

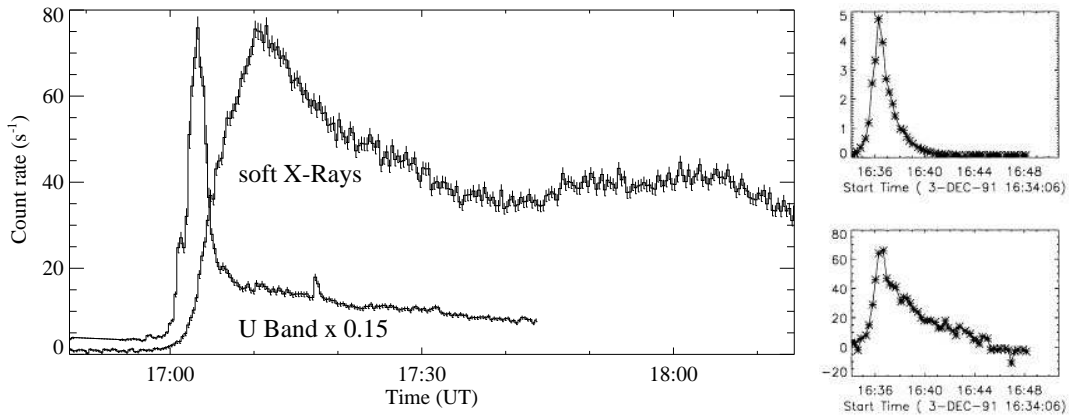


FIGURE 1. Left (a): Large stellar flare on Proxima Cen, showing an initial U-band burst defining the impulsive phase, and a delayed soft X-ray flare defining the gradual phase [18]. - Right (b): Correlation between a solar white light (upper) and a HXR burst (lower panel; from [24]).

with a characteristic delay with respect to the prompt non-thermal emission (Fig. 1a).

HXR emission provides crucial diagnostics for the particle acceleration process in the solar corona and therefore the primary energy release mechanisms (Fig. 1b), yet very little is known about HXR emission from active stars. Detections of a few sources up to several tens of keV with BeppoSAX [10, 35, 11] turn out to be compatible with the extended thermal spectrum also seen in the SXR range. Perhaps the most promising case so far has been reported from Swift observations of the active binary II Peg [34]. During a giant flare, the observed X-ray spectrum up to at least 100 keV is compatible with a power-law electron distribution although a thermal, very hot Maxwellian distribution cannot be excluded.

There is ample complementary evidence for non-thermal electron populations in stellar coronae, including young stellar objects. Radio gyrosynchrotron emission has been detected in many active stars during flares and quiescent periods; the quiescent radio emission correlates with the quiescent SXR radiation, suggesting a causal relation between particle acceleration and heating in the same way as in solar flares [16]. This would suggest the presence of continuous HXR emission as well, as discussed below.

High-energy electrons are also capable of ejecting inner-shell electrons in cool gas, producing the analog of fluorescent emission induced by photon irradiation. Although the 6.4 keV line of “cold iron” occasionally detected in young stellar objects may indeed be from fluorescence in X-ray irradiated circumstellar disks, new evidence suggests a role for electron impact, both in giant flares in evolved stars [34] and in a protostellar flare in which the 6.4 keV line peaked during the rise phase of the soft X-rays [7].

Simbol-X will clarify these issues in detail. Fig. 2a shows a spectral simulation of the II Peg flare [34] as if it had occurred at the distance of the Orion Nebula, exposed for 3 ks. The power-law tail suggested by Osten et al. [34] is included in the model and dominates all emission above ≈ 30 keV. Although such giant flares are exceedingly rare on an individual star, a cluster with > 1000 young stars such as the Orion Nebula Cluster may offer a realistic chance for Simbol-X to study several such events.

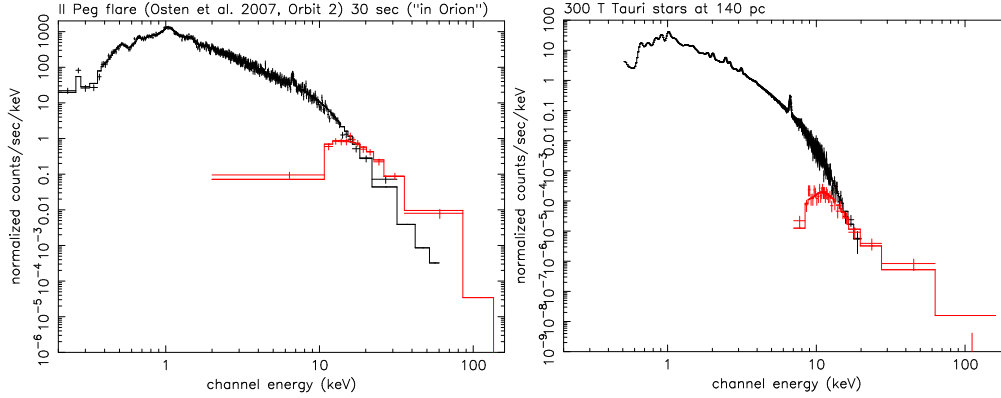


FIGURE 2. Simbol-X simulations. Left (a): II Peg flare [34] at the distance of the Orion Nebula (3 ks of exposure time). Right (b): Summed 200 ks spectrum of 300 typical TTS in Taurus, assuming continuous flaring.

HARD X-RAYS FROM CONTINUOUSLY FLARING CORONAE?

Solar observations show evidence for small-scale flare events occurring in the corona at any time (e.g., [29, 28]). Their distribution in energy follows a power law,

$$\frac{dN}{dE} = kE^{-\alpha} \quad (1)$$

where dN is the number of flares per unit time with a total energy (thermal or radiated) in the interval $[E, E + dE]$. If the power-law index α is ≥ 2 , then the energy integration

$$P_{\text{tot}} = \int_{E_{\text{min}}}^{E_{\text{max}}} \frac{dN}{dE} E dE \approx \frac{k}{\alpha - 2} E_{\text{min}}^{-(\alpha-2)} \quad (2)$$

(assuming $E_{\text{min}} \ll E_{\text{max}}$ and $\alpha > 2$ for the last approximation) diverges for $E_{\text{min}} \rightarrow 0$, i.e., by extrapolating the power law to sufficiently small flare energies, *any* energy release power can be attained [23]. Solar studies have repeatedly resulted in α values on the order of 1.6–1.8 for ordinary solar flares [6] although some statistical investigations suggest $\alpha = 2.0 - 2.6$ for small flares in the quiet solar corona [28, 36]. Stellar studies in the EUV or soft X-ray range have predominantly converged to α between 2 and 3, and this is specifically true for large samples of pre-main sequence stars (e.g., [19, 44]).

An ultimate test of this model would be the detection of continuous hard, non-thermal X-ray emission that should accompany the energy release diagnosed so far in the soft X-ray range (e.g., [32]). I propose in the following a method to estimate the non-thermal hard X-ray production based on some basic relations derived from the Sun and magnetically active stars. For a complementary discussion and application, I refer to Micela & Caramazza [32] and Caramazza et al. [5].

The constant k in Eqns. (1) and (2) can be found from observations of the flare occurrence rate in young, magnetically active stars. The occurrence rate $N(> 10^{32})$ of flares exceeding a radiative soft X-ray output of 10^{32} erg is, for a statistical sample,

$$N(> 10^{32}) \approx 6.9 \times 10^{-34} L_X \quad [\text{s}^{-1}] \quad (3)$$

[2] which agrees within a factor of $\approx 2 - 3$ with the observations of $N(> 10^{32})$ for very active young solar analogs if $\alpha \approx 2 - 2.4$ (as derived from the flare-energy distributions). Note that $N(> 10^{32})$ is proportional to the average soft X-ray luminosity L_X of the star.

Solar soft X-ray flares are accompanied by non-thermal hard X-rays. The respective peak fluxes F_s and F_h are correlated albeit in a non-linear way [4, 26]:

$$F_h = \text{const} F_s^\sigma \quad (4)$$

with $\sigma = 1.2$ [4] or $\sigma = 1.37$ [26]. As F_s refers to the 1.6-12.4 keV channel of the Geostationary Operational Environmental Satellites (GOES), a conversion to the broader soft X-ray range of, say, 0.3-10 keV, is needed; for typical spectra of classical TTS, the GOES flux is about $z = 0.29$ times the total soft X-ray flux. Converting the non-linear relation for measured fluxes at Earth to luminosities of the solar corona, one has

$$L_h = f z^\sigma L_s^\sigma \quad (5)$$

where $f = 2.3 \times 10^{-11}$ (cgs) from the Battaglia et al. [4] study. The effective observation of (quasi-) continuous SXR or HXR emission records the total radiated energy E_s , E_h integrated in time from each flare rather than their peak luminosities. Introducing a characteristic decay time τ_s and τ_h for the soft and hard flare light curve so that $E_{s,h} = \tau_{s,h} L_{s,h}$, one finds for the *average* power in hard X-rays

$$L_H = \int_{E_{h,0}}^{\infty} \frac{dN}{dE_h} E_h dE_h \quad (6)$$

$$= \frac{k}{\alpha - \sigma - 1} \tau_s^{-(\alpha-1)} \tau_h^{(\alpha-1)/\sigma} f^{(\alpha-1)/\sigma} z^{\alpha-1} E_{h,0}^{-(\alpha-\sigma-1)/\sigma} \quad (7)$$

where $E_{h,0}$ is the lowest flare energy required. It can be found by noting that the corresponding $L_{h,0} = f z^\sigma L_{s,0}^\sigma$ and that the integration of the *soft* energies should (according to the flare hypothesis) equal the average soft X-ray luminosity, L_X , from which

$$E_{s,0} = \left[\frac{(\alpha - 2) L_X}{k} \right]^{1/(-\alpha+2)}. \quad (8)$$

After some further manipulations, one finds

$$L_H = \left(6.9 \times 10^{-34} 10^{32(\alpha-1)} \frac{\alpha - 1}{\alpha - 2} \right)^{(1-\sigma)/(2-\alpha)} \frac{\alpha - 2}{\alpha - \sigma - 1} \frac{\tau_h}{\tau_s^\sigma} f z^\sigma L_X. \quad (9)$$

Using parameters from Battaglia et al. [4] ($\sigma = 1.2$, $f = 2.3 \times 10^{-11}$), $z = 0.29$, $\alpha = 2.4$ and reasonable decay times of $\tau_s = 3000$ s and $\tau_h = 1000$ s (see [19] and [26]), one finds $L_H = 8.5 \times 10^{-7} L_X$. Note that in the work by Battaglia et al. [4], the hard X-ray flux is “per keV” at 35 keV. The total hard emission above ≈ 20 keV could reasonably be a factor of perhaps 50 higher, i.e. $L_{H,\text{tot}} \approx 4 \times 10^{-5} L_X$.

Note that $L_H \propto L_X$ despite the non-linearities between flare peak powers in SXR and HXR, although the (different) flare decay times become important. The expected radiation may be easily detectable with Simbol-X from young stellar clusters if a sufficient

number of stars (each assumed to produce equal emission) contribute. Fig. 2b shows a 200 ks simulation for Simbol-X assuming 300 stars with characteristics of an average TTS in the Taurus Molecular Cloud ($L_X = 1.2 \times 10^{30}$ erg s⁻¹, $\alpha = 2.4$) at a distance of 140 pc. Hard radiation can be detected up to 100 keV. The many uncertainties entering the above derivation of course make this an order-of-magnitude estimate only.

REFERENCES

1. C. Argiroffi, G. Micela, and A. Maggio, *Mem.S.A.It.* **79**, 219 (2008).
2. M. Audard, M. Güdel, J. J. Drake, and V. L. Kashyap, *ApJ* **541**, 396 (2000).
3. S. A. Balbus, and J. F. Hawley, *ApJ* **376**, 214 (1991).
4. M. Battaglia, P. C. Grigis, and A. O. Benz, 2005, *A&A* **439**, 737 (2005).
5. M. Caramazza, J. J. Drake, G. Micela, and E. Flaccomio, these proceedings (2009).
6. N. B. Crosby, M. J. Aschwanden, and B. R. Dennis, *Solar Phys.* **143**, 275 (1993).
7. S. Czesla, and J. H. M. M. Schmitt, *A&A* **470**, L13 (2007).
8. B. R. Dennis, *Solar Phys.* **100**, 465 (1985).
9. B. Ercolano, J. J. Drake, J. C. Raymond, and C. C. Clarke, *ApJ* **688**, 398 (2008).
10. F. Favata, and J. H. M. M. Schmitt, *A&A* **350**, 900 (1999).
11. E. Franciosini, R. Pallavicini, and G. Tagliaferri, *A&A* **375**, 196 (2001).
12. K. V. Getman, E. Flaccomio, P. S. Broos, et al., *ApJS* **160**, 319 (2005).
13. G. Giardino, F. Favata, G. Micela, et al., *A&A* **463**, 275 (2007).
14. A. E. Glassgold, J. Najita, and J. Igea, *ApJ* **480**, 344 (1997).
15. A. E. Glassgold, J. Najita, and J. Igea, *ApJ* **615**, 972 (2004).
16. M. Güdel, *ARA&A* **40**, 217 (2002).
17. M. Güdel, and A. Telleschi, *A&A* **474**, L25 (2007).
18. M. Güdel, M. Audard, S. L. Skinner, and M. I. Horvath, *ApJ* **580**, L73 (2002).
19. M. Güdel, M. Audard, V. L. Kashyap, et al., *ApJ* **582**, 423 (2003).
20. M. Güdel, K. R. Briggs, K. Arzner, et al., *A&A* **468**, 353 (2007a).
21. M. Güdel, A. Telleschi, M. Audard, et al., *A&A* **468**, 515 (2007b).
22. K. Hamaguchi, M. F. Corcoran, R. Petre, et al., *ApJ* **623**, 291 (2005).
23. H. S. Hudson, *Solar Phys.* **133**, 357 (1991).
24. H. S. Hudson, L. W. Acton, T. Hirayama, and Y. Uchida, *PASJ* **44**, L77 (1992).
25. K. Imanishi, K. Koyama, and Y. Tsuboi, *ApJ* **557**, 747 (2001).
26. C. Isola, F. Favata, G. Micela, and H. S. Hudson, *A&A* **472**, 261 (2007).
27. J. H. Kastner, D. P. Huenemoerder, N. S. Schulz, et al., *ApJ* **567**, 434 (2002).
28. S. Krucker, and A. O. Benz, *ApJ* **501**, L213 (1998).
29. R. P. Lin, R. A. Schwartz, S. R. Kane, et al., *ApJ* **283**, 421 (1984).
30. R. P. Lin, B. R. Dennis, G. J. Hurford, et al., *Solar Phys.* **210**, 3 (2002).
31. A. Maggio, *Mem.S.A.It.* **79**, 186 (2008).
32. G. Micela, and M. Caramazza, *Mem.S.A.It.* **79**, 266 (2008).
33. G. Micela, F. Favata, G. Giardino, and S. Sciortino, *Mem.S.A.It.* **79**, 264 (2008).
34. R. A. Osten, S. Drake, J. Tueller, et al., *ApJ* **654**, 1052 (2007).
35. R. Pallavicini, G. Tagliaferri, and A. Maggio, *Adv. Space Res.*, **25**, 517 (2000).
36. C. E. Parnell, and P. E. Jupp, *ApJ* **529**, 554 (2000).
37. S. H. Pravdo, E. D. Feigelson, G. Garmire, et al., *Nature*, **413**, 708 (2001).
38. L. Prisinzano, G. Micela, E. Flaccomio, et al., *ApJ* **677**, 401 (2008).
39. T. P. Ray, T. W. B. Muxlow, D. J. Axon, et al., *Nature*, **385**, 415 (1997).
40. S. Sciortino, *Astron. Nachrichten* **329**, 214 (2008a).
41. S. Sciortino, *Mem.S.A.It.* **79**, 192 (2008b).
42. K. Smith, M. Pestalozzi, M. Güdel, et al., *A&A* **406**, 957 (2003).
43. P. Stäuber, J. K. Jorgensen, E. F. van Dishoeck, et al., *A&A* **453**, 555 (2006).
44. B. Stelzer, E. Flaccomio, K. Briggs, et al., *A&A* **468**, 463 (2007).
45. A. Telleschi, M. Güdel, K. R. Briggs, et al., *A&A* **468**, 425 (2007).